Plasma Dynamics

18. Plasma Dynamics

Academic and Research Staff

Prof. G. Bekefi, Prof. A. Bers, Prof. B. Coppi, Prof. T.H. Dupree, Prof. L.M. Lidsky, Prof. J.E. McCune, Prof. M. Porkolab, Prof. L.D. Smullin, Dr. R.H. Berman, Dr. G. Bertin, Dr. P.T. Bonoli, Dr. T. Boutros-Ghali, Dr. K-I. Chen, Dr. R.C. Englade, Dr. V. Fuchs[6], Dr. D. Hewett[7], Dr. K. Hizanides, Dr. J.H. Irby, Dr. V.B. Krapchev, Dr. J.S. Levine, Dr. S.C. Luckhardt, Dr. P.A. Politzer, Dr. A.K. Ram, Dr. J. Ramos, Dr. M.E. Read, Dr. N.N. Sharky, Dr. R.E. Shefer, Dr. L.E. Sugiyama, Dr. D.J. Tetreault, E.W. Fitzgerald, R. Li, I. Mastovsky, Y.Z. Yin, M.-L. Xue.

Graduate Students

J.G. Aspinall, P.E. Cavoulacos, K.D. Cogswell, G.B. Crew, J. Fajans, A.S. Fisher, M.E. Foord, G. Francis, R.C. Garner, T.R. Gentile, P.J. Gierszewski, K.E. Hackett, A.M. Hamza, L.P. Harten, D. Hinshelwood, D.A. Humphreys, K.D. Jacob, M. Kanapathipillai, D.A. Kirkpatrick, S.F. Knowlton, B.L. LaBombard, W.P. Marable, J.J. Martinell, M.E. Mauel, M.J. Mayberry, F.S. McDermott, A. Pachtman, Y. Pu, C.M. Rappaport, R.R. Rohatgi, S.E. Rowley, D.R. Thayer, S.H. Voldman

18.1 Relativistic Electron Beams and Generation of Coherent Electromagnetic Radiation

National Science Foundation (Grants ECS82-00646 and ECS82-13485)
U.S. Air Force - Office of Scientific Research (Contracts F33615-81-K-1426, F49620-83-C-0008, and AFOSR-84-0026)
U.S. Navy - Office of Naval Research (Contract N00014-83-K-2024)
Sandia National Laboratory (Contracts 31-5606 and 48-5725)
George Bekefi, Ruth E. Shefer

Relativistic electron beam research at M.I.T. focuses on the generation of intense coherent electromagnetic radiation in the centimeter, millimeter and submillimeter wavelength ranges. The primary radiation mechanism which is being studied at the present time is the free electron laser instability which is excited when an electron beam passes through a spatially periodic, transverse magnetic field (wiggler field). This instability is characterized by axial electron bunching and has emission wavelengths associated with the Doppler upshifted wiggler periodicity.

---

[6] IREQ-Hydro Quebec, Montreal, Canada

[7] Plasma Fusion Center, M.I.T.

Intense coherent sources of centimeter and millimeter wavelength radiation find applications in many diverse fields of research and technology including heating and diagnostics of thermonuclear fusion plasmas, photochemistry, solid state physics, and biophysics. One advantage of free electron systems such as the free electron laser are the very high predicted efficiencies which may be attained. Another important advantage is frequency tunability which results from the fact that the radiation frequency is not locked to an atomic or molecular transition or to an electromagnetic mode of a resonant structure but is instead determined by the velocity of the beam electrons.

The experimental facilities available to this group include three pulsed high voltage accelerators capable of delivering up to 100 kA of current at 0.5 to 1.5 MV. Their characteristics are summarized below:

Pulserad 110 A	
Voltage	1.5 MV
Current	20 kA
Pulse Length	30 ns
Pulserad 615 MR	
Voltage	0.5 MV
Current	4 kA
Pulse Length	1μs
Nereus	
Voltage	0.6 MV
Current	100 kA
Pulse Length	30 ns

In the following sections, various radiation generation experiments presently being carried using the above electron beam generators are discussed.

a. The Rippled Field Magnetron (Cross-Field Free Electron Laser)

To achieve efficient conversion of energy from a stream of free electrons to electromagnetic radiation, near synchronism must be attained between the velocity of the electrons and the phase velocity of the wave. In cross-field devices, of which the magnetron is a typical example, this synchronism occurs between electrons undergoing a $v = \vec{E}_o \times \vec{B}_o$ drift in orthogonal electric and magnetic fields, and an electromagnetic wave whose velocity is reduced by a slow-wave structure comprised of a periodic assembly of resonant cavities. The complex system of closely spaced resonators embedded in the anode block limits the conventional magnetron to wavelengths in the centimeter range. Moreover, at high voltages typical of relativistic magnetrons, RF or dc breakdown in the electron beam interaction space, and at the sharp resonator edges poses serious problems.

The rippled-field magnetron is a novel source of coherent radiation devoid of physical slow-wave structures and capable of radiating at much higher frequencies than a conventional magnetron. The

configuration of the anode and cathode is similar to the so-called "smooth-bore" magnetron, but it differs from the latter in that the electrons are subjected to an additional field, an azimuthally periodic (wiggler) magnetic field B_ω oriented transversely to the flow velocity v. The resulting $-e\vec{v} \times \vec{B}_\omega$ force gives the electrons an undulatory motion which effectively increases their velocity, and allows them to become synchronous with one of the fast TE or TM electromagnetic modes (phase velocity > c) characteristic of the smooth-bore magnetron.

The magnetron configuration is cylindrical rather than linear as in conventional FEL's, and the system is therefore very compact. The cylindrical geometry also allows for a continuous circulation of the growing electromagnetic wave, and because of this internal feedback, the rippled-field magnetron is basically an oscillator rather than an amplifier as is the case of the FEL.

We have obtained measurements of millimeter-wave emission from the rippled field magnetron.[1] In these experiments the magnetic wiggler field is produced by a periodic assembly of samarium-cobalt bar magnets positioned behind the smooth, stainless steel electrodes. Maximum radiated power in the 26.5-60 GHz frequency band is obtained with a wiggler periodicity of 2.53 cm and a wiggler field amplitude of 1.96 kG. Under these conditions a narrow band spectral line is observed with a line width at the half power points of less than 2.2 GHz. The center frequency of this line can be varied from 32 GHz to 46 GHz by varying B_z between 5.8 kG and 9 kG. No deterioration in line profile is observed over this range. The total radiated power above 26.5 GHz measured with this wiggler is 300 kW; which is more than a factor of thirty above the broadband noise observed with no wiggler.

We note that this device differs from the conventional FEL in that the electron source (the cathode) and the acceleration region (the anode-cathode gap) are integral parts of the RF interaction space. This makes for high space-charge densities which result in large growth rates of the instability; but it has the disadvantages that the current density and position of the interacting electrons in the gap are difficult to control. In the section below we describe an experiment in which a thin, hollow rotating electron beam is injected into the cylindrical wiggler structure. This configuration eliminates the need for the accelerating anode-cathode electric field E_o and allows us to easily control both the current density and the beam dynamics in the interaction gap.

b. A Rotating Beam Free Electron Laser

In this section we describe a variation on the rippled field magnetron in which a rotating electron beam interacts with a rippled magnetic field.[2] This work is being carried out at the University of Maryland in collaboration with Prof. W.W. Destler.

In the experiments, a 12 cm diameter, hollow, rotating electron beam (2 MeV, 1-2 kA, 5 ns) is generated by passing a hollow non-rotating beam through a narrow magnetic cusp. The rotating beam performs helical orbits ($\beta_\theta \simeq .95$, $\beta_z \simeq .2$) downstream of the cusp in an axial guide field of about 1450 Gauss. Radiation is produced by the interaction of the beam with an azimuthally periodic wiggler magnetic field produced by samarium cobalt magnets located interior and exterior to the

beam. In the present work, the wiggler field has an amplitude of about 1300 Gauss, six spatial periods around the azimuth, and a periodicity of 6.28 cm.

We have observed at least 200 kW of radiation above 91 GHz in initial experiments, a result consistent with the frequency expected for a linear free electron laser operating with comparable parameters. Radiation at these frequencies is not observed in the absence of the wiggler field. Numerical calculations of the electron orbits in the combined axial and wiggler fields indicate that the orbits are relatively unperturbed in the r-Θ plane and that the perturbation of the orbits due to the wiggler is primarily axial, as desired. Measurements of the actual circulating current exciting the wiggler region with and without the wiggler magnets in place confirm that the wiggler field does not have a seriously adverse effect on the electron orbits.

Measurements of the radiation spectrum using a grating spectrometer and studies of the effects of wiggler amplitude and periodicity are currently underway.

c. A Low Voltage Free Electron Laser

Many theoretical studies have been devoted to free electron lasers comprised of an electron stream traversing a periodic, circularly polarized magnetic (wiggler) field, as can be generated with bifilar, helical, current-carrying wires. The electron dynamics in these systems exhibit simple properties that have considerable theoretical appeal. However, from the experimental point of view large amplitude, circularly polarized wiggler fields are difficult to attain because of the large currents that are required in their windings; and for long pulse or steady-state operation, bifilar conductors may be entirely out of the question. In view of the above, studies of free electron lasers have begun in which the electron beam is subjected to a periodic, linearly polarized transverse magnetic field such as can be produced, for example, by an assembly of permanent magnets.

An experiment is underway to investigate the microwave and electron beam characteristics of a Free Electron Laser amplifier using a linear wiggler field. In this experiment, a 35 keV, 1A electron beam is produced by a thermionic cathode. The beam pulse width is 1-5 μsec, with a 0.001 duty cycle. A guiding axial magnetic field, generated by a series of D.C. powered, water cooled solenoid coils, is variable up to a maximum of B_o = 3 kG. This field both prevents radial expansion of the beam and allows investigation of the FEL gain near the cyclotron resonance condition, $k_o V_z - \Omega_o/\gamma = 0$. ($K_o = 2\pi/\ell$, ℓ = wiggler period, $\Omega_o = (eB_o/m_o)$, $\gamma = (1 - \beta^2)^{-1/2}$). When this resonance condition is satisfied, the cyclotron wavelength of an electron in the uniform guiding magnetic field equals the wiggler periodicity. Enhanced growth of the radiation field is predicted as this condition is approached.

A set of 480 samarium cobalt permanent magnets produces a linearly polarized wiggler magnetic field. The wiggler is 60 periods long, with periodicity ℓ = 2.0 cm. The wiggler amplitude is variable from 0.1 to 1.0 kG.

The beam drift tube is a length of WR-137 band rectangular waveguide. The 6 GHz FEL output frequency lies in the lowest (TE_{10}) mode of the waveguide. A calibrated crystal detector and a conventional spectrum analyzer are used to make microwave power and frequency measurements. Determination of the electron beam axial velocity distribution is made using a gridded Faraday cup. At these low beam voltages, it is possible to use a repelling grid in the cup. Measurement of the beam properties and the microwaves can be made simultaneously.

d. An Intermediate Energy, Long Pulse Free Electron Laser

An intermediate energy free electron laser experiment designed to investigate cyclotron resonance effects is being carried out on the Pulserad 615 MR electron beam facility. The experimental parameters are given in the table below:

Beam Energy (keV)	150–200
Beam Current Density ($A\text{–}cm^{-2}$)	70
Pulse Length (μs)	2
Axial Magnetic Field (kG)	0.7–7.0
Wiggler Field Amplitude (kG)	0–1.5
Wiggler Period (cm)	3.3
Number of Periods	50

The Pulserad 615 MR power source is a Marx generator which produces a repeatable, flat accelerating voltage pulse. It has the capability of operating with a thermionic (hot cathode) electron gun. In this experiment the thermionic cathode is immersed in a shaped focusing magnetic field. The perpendicular energy of the emitted electrons is estimated to be less than one percent of their total energy. This characteristic of the electron beam is important in free electron devices from the standpoint of producing coherent radiation with high efficiency.

The beam propagates in a two meter long drift tube, guided by a uniform axial magnetic field that can be varied between 0.7 and 7.0 kG. The wiggler fields are generated by a bifilar helical winding. An adjustable, adiabatic entrance profile is produced by staggering the wiggler termination windings.[3] This termination scheme allows us to increase the wiggler field amplitude to its full value slowly and with any amplitude profile desired at the upstream end of the wiggler. Computer simulations have shown that the entrance profile is very important in preserving low beam energy spread in both the transverse and axial directions as the beam enters the wiggler field. The system has been designed so that under normal operating conditions, the emitted radiation propagates in the lowest mode of the cylindrical drift tube.

We have observed microwave power levels of over 10 kW at approximately 10 GHz. Spectra observed with an X-band waveguide dispersive line show that most of the power is concentrated in a narrow peak ($\Delta f/f < .01$). Preliminary results indicate that the output frequency increases with beam energy with the functional form predicted by theory.

Measurements of the beam current have been made in the vicinity of the resonance $k_w v_o = \Omega_o$ that occurs when the cyclotron frequency of the guide magnetic field equals the frequency $k_w v_o$ associated with the wiggler (k_w = wiggler wave number). As the axial magnetic field is increased and passes through the resonance, the beam current transmitted through the wiggler drops sharply. Beyond this point, the current increases slowly to its original value. Measurements of microwave power levels and spectra near resonance are underway.

e. A Submillimeter Free Electron Laser using a High Quality Electron Beam

In this experiment, a high current density, high energy electron beam is used to produce submillimeter wavelength radiation. The measured parameters of the electron beam are:

Beam Voltage	1.6 MV
Beam Current Density	200 A-cm^{-2}
Axial Momentum Spread	$\leq$ 1%

Other experimental parameters are as follows:

Wiggler Period	2.0 cm
Number of Periods	50
Wiggler Field Amplitude	1200 Gauss
Output Frequency	456 GHz
Theoretical Single Pass Gain	23 dB
Saturated Efficiency	0.75%

The M.I.T. Pulserad 110A accelerator facility is used in conjunction with a five stage electrostatically focused field emission electron gun to produce a high quality intense relativistic electron beam. The beam is then guided into a bifilar helical wiggler field by means of a short solenoidal coil which acts as a focusing lens. The coil is positioned upstream of the wiggler and obviates the necessity of having a guiding magnetic field in the wiggler region. The lack of a guide field in the wiggler region eliminates the possibility of exciting the cyclotron maser instability.

The beam quality has been determined by measurements of beam emittance and beam momentum spread.[4] Emittance measurements were carried out by allowing the beam to impinge on an array of pinholes in a brass disk, and then observing the transmitted beamlets on a fluorescent screen at a known distance downstream. We find that the normalized emittance is $\leq$ 50 mr-cm. Beam momentum spread measurements were carried out using a magnetic spectrometer. The spectrometer is of the Browne-Buechner type and is capable of a resolution in $\gamma v_{\parallel}$ of less than 0.1%. Both time integrated and time resolved measurements carried out on this electron beam show an axial momentum spread of less than one percent.

References

1. G. Bekefi, R.E. Shefer, and B.D. Nevins, Proc. Int. Conf. on Lasers '82, in R.C. Powell (Ed.) (STS Press, McLean, Virginia 1982), p. 136.

2. G. Bekefi, R.E. Shefer, and W.W. Destler, Appl. Phys. Lett. 44, 280 (1984).
3. J. Fajans, J. Appl. Phys. 55, Jan. 1, 1984.
4. R.E. Shefer, D.A. Kirkpatrick, and G. Bekefi, Bull. Am. Phys. Soc. 28, 1063 (1983).

18.2 Tokamak Research: RF Heating and Current Drive

U.S. Department of Energy (Contract DE-AC02-78ET-51013)

George Bekefi, Miklos Porkolab, Kuo-in Chen, Stanley C. Luckhardt

The main theme of the Versator II program is to understand interactions between externally excited lower-hybrid waves and tokamak plasmas. For typical tokamak plasmas, the lower-hybrid wave has a frequency in the range of a few hundred MHz to a few GHz. In current experiments, the lower-hybrid wave is generated by a RF system which consists of a 150 kW, 800 MHz klystron, and a waveguide power splitter with four output channels. The phase of each output can be continuously adjusted (0° ~ 360°) with mechanical phase shifters. Such phase control allows traveling wave spectra to be launched either parallel or antiparallel to the direction of the electron ohmic drift, $\Delta\Phi = \pm 90°$, or a standing wave spectrum can be excited with $\Delta\Phi = 180°$.

Versator II is a medium-size tokamak with the following important physical and plasma parameters: major radius R = 40.5 cm, limiter radius a = 13 cm, toroidal field B_T ~ (8–15) kG, plasma current I_p ~ (30–60) kA, discharge length τ_{pulse} ~ (30–40) ms, central electron temperature T_{eo} ~ (250–450) eV, central ion temperature T_{io} ~ (120–180) eV, line average density $\bar{n}_e$ ~ (0.1–3) x $10^{13} cm^{-3}$ and Z_{eff} ~ 2.

The phase velocity of the lower-hybrid wave can be controlled by adjusting phases between launching waveguides. With proper phase velocity and plasma parameters (e.g., density, toroidal magnetic field, etc.), the lower-hybrid wave will interact with either plasma electrons or ions. Consequently, the physics problems of heating (electron or ion) and current generation by lower-hybrid waves can be studied.

The emphases of these experiments in 1983 are on the toroidal effects of wave penetration; by making a comparison of launching waves through a top port and a side port at the same toroidal position. Important experimental results and detailed diagnostic measurements are summarized below.

Present Status

18.3 I. Lower-Hybrid Current Drive (LHCD) Experiment

18.3.1 Top Launching vs. Side Launching

Ray tracing theory[1] has shown that traveling waves launched from the top of the torus in the direction $\hat{S} = \vec{B_T} \cdot \vec{I_p} \hat{\Phi} / |B_T||I_p|$ (where $\hat{\Phi}$ is the toroidal unit vector) experience an upshift in their $n_{\parallel} (= ck_{\parallel}/\omega)$ due to toroidal effects. Generally, for top launching in the $+\hat{S}$ direction, the wave slows down along field lines and is often absorbed in the first poloidal transit through the center of the plasma. However, when waves are launched from the midplane on the outside, $n_{\parallel}$ downshifted initially, making first pass absorption less likely due to the difficulty in satisfying the Landau resonance condition. In general, top launching is expected to give improved power absorption efficiency and an interaction with lower energy electron when compared with side launching. Measurement of comparative current drive efficiency with couplers mounted on the top and side of the torus therefore appears to be a test of the ray tracing prediction of toroidal shifts in $n_{\parallel}$. Nevertheless, it should be noted that according to a very simple picture of Fisch current drive theory,[2] the merit factor of current drive $I_{RF}/P_{RF} \propto 1/n_{\parallel}^2$, so the $n_{\parallel}$ upshift is expected to result in reduced current drive efficiency.

Table 1

	4-Guide Top	4-Guide Side	6-Guide Side
$\Delta\Phi$	+90°	+90°	+90°
$N_{\parallel o}^{PEAK}$	8	8	8
$\bar{n}_e$	$4\times10^{12}cm^{-3}$	$4\times10^{12}cm^{-3}$	$4\times10^{12}cm^{-3}$
I_p	36 kA	36 kA	32 kA
P_{NET}	13 kW	11 kW	8 kW
ΔI	3.0 kA	5.3 kA	3.5 kA
Δt	5 msec	5 msec	5 msec
$\tau_{L/R} \simeq$	15 msec	15 msec	15 msec
$I_{RF} \simeq \frac{\Delta I}{\Delta t} \tau_{L/R}$	9.0 kA	16 kA	13 kA
$S = \bar{n}_{15} \frac{R_o I_{RF}}{P_{NET}}$	0.11	0.23	0.26

A comparison of current drive efficiencies between side and top launching experiments

The basic experiment results are shown in Table 1 where comparison is made in terms of the scaling parameter S defined as $S = (I_{RF}/P_{NET})\,\bar{n}_{15}R_0$. It appears from these initial experiments that the side couplers have a factor of 2–3 higher current drive efficiency than the top couplers. This reduction in S may be caused by the toroidal effects on $n_{\parallel}$ predicted by ray tracing theory.

18.3.2 Particle Confinement

Observed density increases during LHCD experiments have been investigated in detail in 1983. These density increases can possibly be caused either by extra influxes of neutral hydrogen and impurities or improved confinement produced by the RF. Spectroscopically, we have measured emissions of neutral hydrogen and impurities. Specifically, H_α emission is found to decrease; thus, the increased density is not the result of increased ionization of hydrogen and impurities.

The global particle balance equation $(dN_e/dt) = S - (N_e/\tau_p)$ (where N_e is the total number of electrons in the plasma, S is the source term, τ_p is the global particle confinement time) is used to deduce τ_p (see Fig. 18–1).

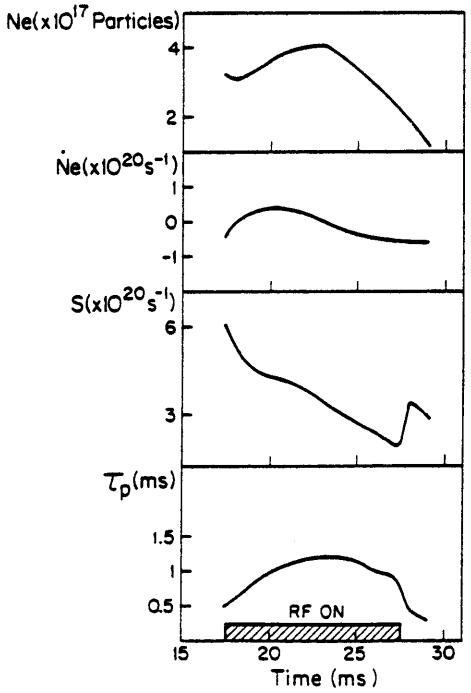

Figure 18-1: Analysis of global particle confinement

It appears the τ_p increases by approximately a factor of two during LHCD. This increase is

correlated with stabilization of the Parail–Pogutse runaway tail mode. This mode is normally present during low density ohmic discharges, and can be stabilized during RF current drive. When the instability does occur during the RF phase, the density suddenly decreases.

18.3.3 Current Profiles

Current profile changes can induce toroidal loop voltages inside the plasma, produce additional current, and complicate the interpretation of the current drive data. Therefore, a detailed study of current profile behavior during LHCD was carried out. One way to obtain information about the current profile is to do the analysis of the plasma equilibrium data. This analysis gives the time dependence of the quantity $\ell_i/2 + \beta_\theta$ (where ℓ_i is the internal inductance and β_θ the poloidal β value) through the Shafranov equilibrium condition. In the current drive density regime, β_θ is usually taken as small compared to $\ell_i/2$ so the data analysis gives essentially the time dependence of $\ell_i/2$. Increases in ℓ_i indicate the current profile is becoming more peaked and decreases indicate the current profile is flattening.

In the low density ohmic discharges we find that the value of ℓ_i is typically 2–3, and increases slowly as plasma current decays near the end of the discharge. During LHCD, the measurement shows that the current profile is essentially the same as that of the ohmic plasma and that internally induced voltages do not constitute significantly to the current in the Versator current drive experiment. Calculations of ℓ_i from model current profiles indicate that the current is peaked on axis with a radius of ~ 4 cm, r/a ~ 0.3.

Another way to obtain information on current profiles is to measure spatial profile of hard x–ray emissions from the plasma. Hard x–ray measurements have shown a very peaked spatial profile (FWHM ~ 6 cm or possibly smaller) before and during LHCD. This profile measurement seems to be consistent with previous $\ell_i/2 + \beta_\theta$ measurements.

18.3.4 Density Fluctuations and Wave Propagation

The microwave scattering experiment on Versator II uses scattering of a 140 GHz beam to measure density fluctuations. This experiment has been active, looking at both low–frequency fluctuations (20–500 kHz) thought to be associated with transport, and, more recently, the externally–driven 800 MHz lower–hybrid wave. The low–frequency fluctuations have been studied during LHCD; exponential frequency spectra have been measured. During current–drive the spectra are found to steepen as the density fluctuations (at fixed wavevector 7 cm^{-1}) decrease. The scattering experiment is now being used to detect the 800 MHz lower–hybrid wave, which is externally launched by a phased waveguide grill. To date a clean signal has been obtained and the wave has been observed. These experiments will continue in an attempt to study the propagation of the lower–hybrid wave in Versator plasmas.

18.3.5 Bulk and Tail Electrons

Soft and hard x-ray pulse height analysis (PHA) diagnostics are routinely used on Versator II to study the behavior of the superthermal electron tail during lower-hybrid current drive and heating experiments. A Si(Li) detector soft x-ray (1-30 keV) diagnostic is capable of radially scanning the entire plasma cross section from the side while a 3" x 3" NaI(Tℓ) hard x-ray (20 keV-1 MeV) detector can scan the entire plasma cross section from below. Measurements in the low density LHCD regime ($\bar{n}_e \lesssim 6 \times 10^{12}$ cm^{-3}) show the presence of a high energy electron tail with maximum detected energies exceeding 300 keV, located in the central 5 cm of the 26 cm diameter plasma.

Time resolved measurements of soft and hard x-rays have shown a strong bursting behavior which correlates with the Parail-Pogutse runaway tail mode instability routinely observed in the low density current drive regime (see Fig. 18-2). The x-ray bursts originate from the central region of the plasma, but are much stronger in the top half of the plasma suggesting the possibility of ripple trapping of some electrons when they are pitch angle scattered from the parallel to the perpendicular direction by the instability. Future experiments will take place after the Versator upgrade is complete, and this will allow the OH electric field to be eliminated during current drive. Then, an attempt will be made to measure the anisotropy of the high energy RF sustained electron tail by scanning a NaI(Tℓ) detector in angle with respect to the magnetic field.

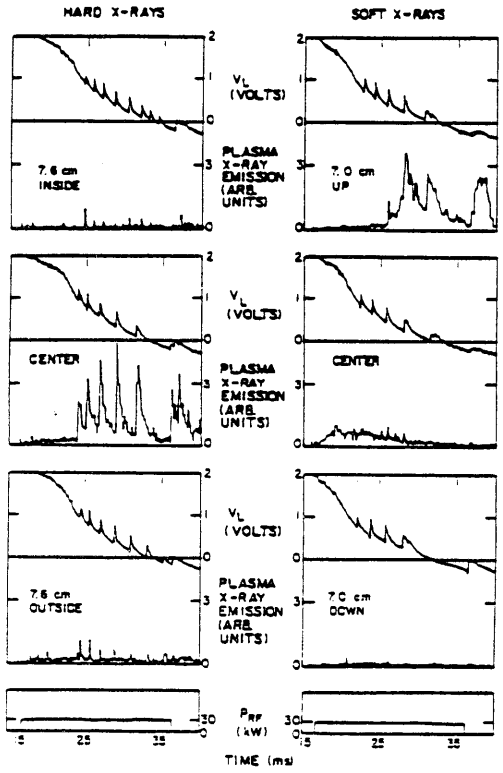

Figure 18-2: Parail-Pogutse instability observed by hard and soft x-ray diagnostics during LHCD

At higher densities, in the theoretical electron heating regime ($8 \times 10^{12} \lesssim \bar{n}_e \lesssim 1.5 \times 10^{13}$), a clear enhancement (up to x10) of the soft x-ray superthermal tail (4–25 keV) is observed. Under these conditions, the Parail–Pogutse instabilitiy is not usually present, either with or without RF. However, the electron temperature, obtained by fitting the slope of the continuum soft x-ray spectrum, does not change during RF injection. This result is confirmed by Thomson scattering measurements. Future experiments are needed to explain why the RF generated electron tail is not sufficient to thermalize with bulk electrons to produce bulk heating in this density regime.

18.3.6 $\omega < \omega_{pe}$ Emission Measurements

Emissions in frequency range from 1 GHz to 12.4 GHz have been measured during LHCD by a high frequency probe located behind the limiter radius. The signal is composed of a slowly varying "background" signal plus periodic bursting signals which are due to the waves driven unstable by the presence of an anisotropic tail of runaway electrons. The constant background signal ($f < 4$ GHz) during discharges with LHRF goes up by 10 dB compared to ohmic discharges (see Fig. 18–3). The frequency spectrum of bursting signals is broadened (significant signal extended out to 12 GHz) during LHCD compared to ohmic discharges (< 6 GHz) (see Fig. 18–4). The burst period is also changed from (0.25 ms–1 ms) for the ohmic case to (1 ms–3 ms) for the RF case. The frequency spectra of these bursting signals seems to be consistent with a theoretical model[3] in which waves are driven unstable at the anomalous Doppler resonance which only weakly damped at the Cerenkov resonance.

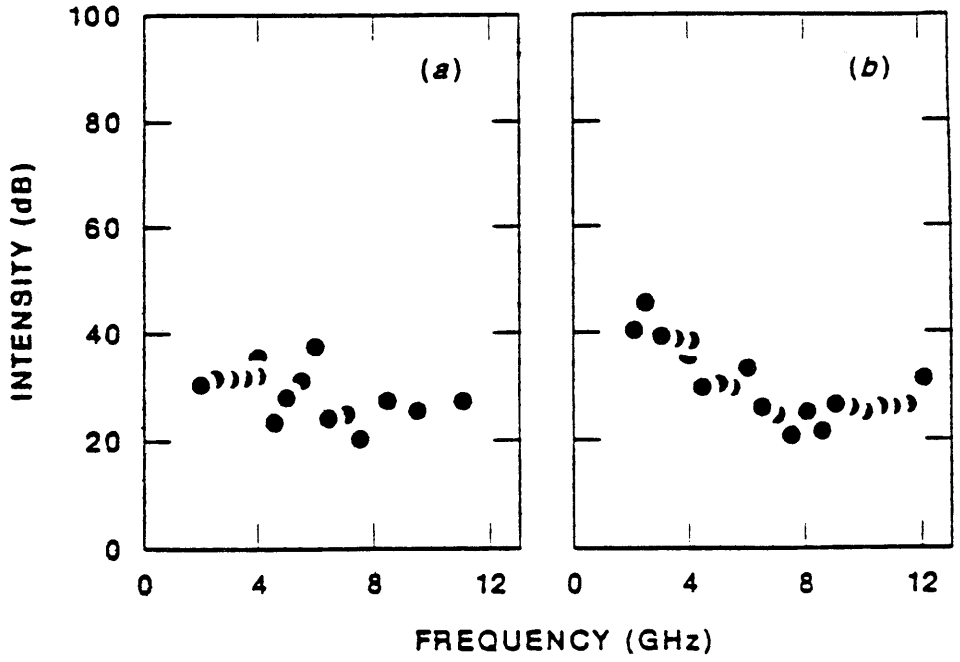

Figure 18-3: Spectra of the steady background emission at $\bar{n}_e = 4.5 \times 10^{12} cm^{-3}$ for (a) Ohmic (b) LHCD discharges

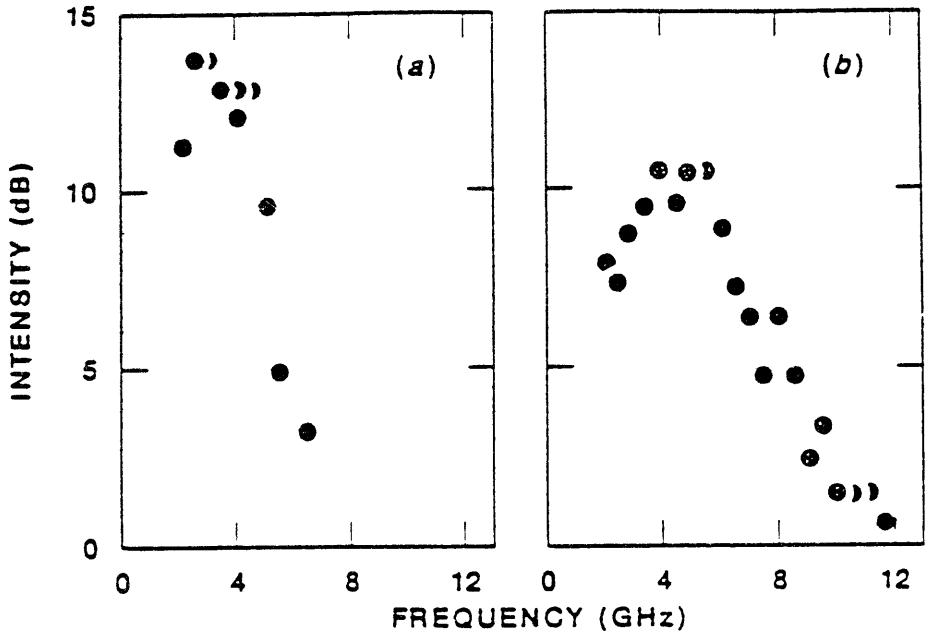

Figure 18-4: Spectra of the intense bursts of emission plotted in dB above the background emission level of $\bar{n}_e = 4.5 \times 10^{12} cm^{-3}$ for (a) Ohmic (b) LHCD discharges

II. Lower-Hybrid Ion Heating (LHH) Experiments

In ion heating studies encompassing the density range $1.3 \times 10^{13} cm^{-3} \leq n_e \leq 3.2 \times 10^{13} cm^{-3}$, no bulk heating of ion population was observed by UV Doppler broadening measurements during RF injection with the top-launching antenna for any value of the phase angle between waveguides ($45° \leq |\Delta\Phi| \leq 180°$). On the other hand, the perpendicular neutral charge-exchange flux showed a strong increase with RF injection. As in the case of side-launch injection, the decay of the neutral flux enhancement was no more than 150 μs following the shutoff of the RF power. The apparent temperature increase is dependent on the relative phase between waveguides, with the larger increases occurring at lower phase angles. The time-evolutions of the ion temperature inferred from perpendicular charge-exchange and UV measurements are shown in Fig. 18-5 for $\Delta\Phi = \pm 90°$ and 180° at $P_{RF} = 100$ kW and $\bar{n}_e = 2.6 \times 10^{13} cm^{-3}$

The apparent ion temperature increase indicated by the charge-exchange measurements is not believed to represent an actual increase in the bulk temperature, but most likely results from the presence of an ion tail near the edge of the plasma. The enhancement of the 0.5-1.0 keV neutral flux during RF injection with the top-launcher is consistent with the damping of higher $n_\parallel$ waves in the experiment (but it is in contrast with earlier side launcher studies). The larger $n_\parallel$ values at the damping locations may result from the higher average $n_\parallel$ spectrum launched by the narrow-waveguide top-launcher, and not necessarily from an upshift in $n_\parallel$ due to toroidal effects. The symmetry of the charge-exchange spectrum with $\Delta\Phi$ along with the lack of bulk ion heating

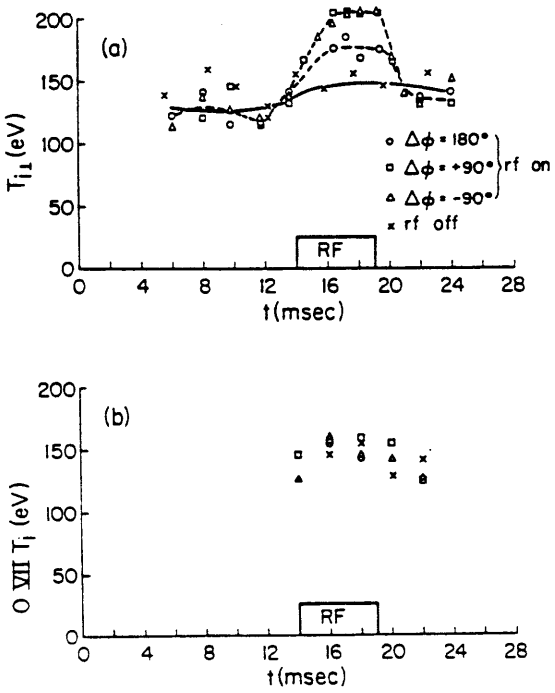

Figure 18-5: Temporal evolution of the central ion temperature during rf injection with the top–launcher

indicated by UV spectroscopic measurements is not consistent with the linear damping mechanism assumed in the ray–tracing calculations. Damping of parametric decay waves near the plasma edge may again be responsible for the observed effects on the ion energy spectrum. Consequently, the results of top–launching experiments can neither support nor refute the predictions of toroidal ray–tracing theory as it applies to lower–hybrid ion heating.

18.4 $2\omega_{ce}$ Emission and Absorption Experiments in ISX–B Tokamak

These experiments are under a joint project between the Versator II group and the ISX–B group at the Oak Ridge National Laboratory. The first goal of these measurements is to demonstrate that $2\omega_{ce}$ emissions can be used as a reliable diagnostic to measure electron temperature temporally and spatially. Secondly, to measure the absorption coefficient of $2\omega_{ce}$ extraordinary mode in a thermalized plasma accurately, so the measurement can be compared with analytic theoretical calculations and numerical model simulation results. This comparison is relevant in terms of planning future electron cyclotron heating experiments.

For studies of extraordinary mode emission at $\omega = 2\omega_{ce}$, the plasma is optically thick and $\omega = 2\omega_{ce}$ emission is approximately at the blackbody level. Electron temperatures at three spatial locations deduced from local $2\omega_{ce}$ emissions are shown in Fig. 18–6 for a typical neutral beam heated ISX–B discharge.

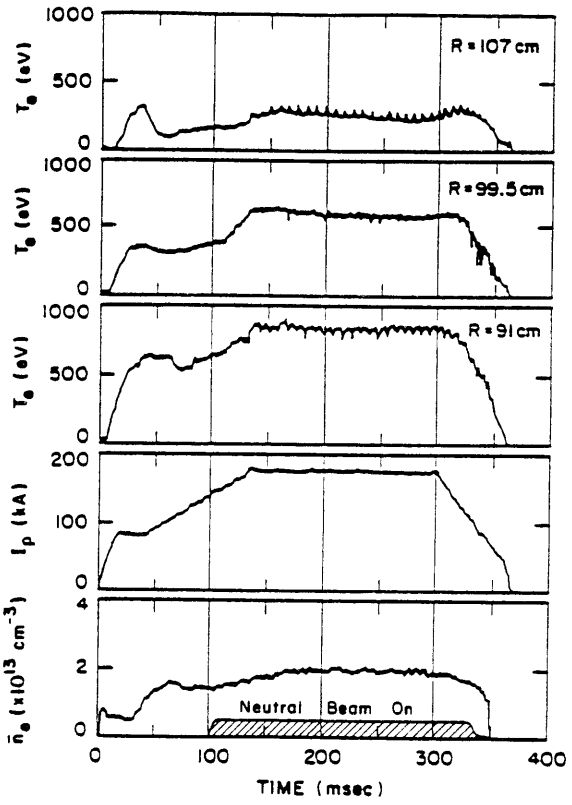

Figure 18-6: The electron temperature, Te, derived from $2\omega_{ce}$ emission for a typical neutral beam heated ISX-B discharge at B_o = 13.1 kG.

For the absorption measurement a transmitting antenna located on the high field side of the ISX-B vacuum vessel launches a wave along the equatorial plane of the torus and polarized in the extraordinary mode. The wave can be partially absorbed at the $\omega = 2\omega_{ce}$ layer. After passing through the plasma, the transmitted intensity is monitored by a receiving antenna located opposite on the low field side of the torus. By taking the diffraction of the input beam into account the absorption coefficient can be calculated from the input power and measured transmitted power. These absorption measurements are in good agreement with the analytic calculation of Ref. 4 and with the predictions of a fully relativistic numerical simulation developed by an Oak Ridge theory group.

References

1. P.T. Bonoli, E. Ott, Phys. Fluids 25, 359 (1982).
2. N.J. Fisch, Phys. Rev. Lett. 41, 873 (1978).
3. V.V. Parail, O.P. Pogutse, Nucl. Fusion 18, 303 (1978).
4. T.M. Antonsen, W. Manheimer, Phys. Fluids 21, 2295 (1978).

18.5 Nonlinear Wave Interactions—RF Heating and Current Generation in Plasmas

National Science Foundation (Grants ECS82-00646 and ECS82-13430)
U.S. Department of Energy (Contract DE-AC02-78-ET-51013)
U.S. Air Force - Office of Scientific Research (Contract F33615-81K-1426)
Abraham Bers, Vladimir Fuchs[8], Dennis Hewett[9], Kyriakos Hizanidis, Vladimir Krapchev, Abhay Ram, Gregory Francis, Leo Harten

The work and objectives of this theoretical and computational group were described in the RLE Progress Report No. 124, January 1982, pp. 112–113.

In the following seven subsections we report on our accomplishments of the past year on the following problems:

A. Theoretical modeling and analyses of current generation by lower-hybrid waves (subsections a and b). As described in our progress report of last year, this work is directly related to ongoing experimental efforts to produce a steady-state current for plasma confinement in toroidal geometry with the use of externally applied microwave power. More generally, this work seeks to understand the steady-states of high-temperature plasmas that are driven by RF waves.

B. Induced stochasticity in the dynamics of plasma particles by RF fields (subsections c and d). This work is part of our continuing studies of the nonlinear wave-particle interactions in a plasma. The important, new result reported in (d) is that an appropriately frequency modulated wave can induce stochastic motion in particles whose velocity is very different from the phase velocities of the wave fields, and at field amplitudes that are very much lower than those required for a single frequency wave.

C. Space-time evolution of relativistic instabilities (subsections e and f). Here we report on success in generalizing the absolute vs. convective instability analysis to include relativistic-electromagnetic interactions in plasmas. The applications of this work are to understanding instabilities in intensely heated plasmas by electron cyclotron RF power, and to explore the possibility of gyrotron-like devices at harmonics of the electron cyclotron frequency.

a. Theory of Lower-Hybrid Current Generation

The linearized, steady state, two-dimensional Fokker-Planck equation for electrons in the presence of strong RF diffusion has been solved analytically and the results have been compared with a

[8]Visiting Scientist from IREQ - Hydroquebec, Montreal, Canada

[9]Plasma Fusion Center, M.I.T., now at LLNL, Livermore, California

numerical integration of the equations. In this case the diffusion coefficient $D \equiv D_{QL}/\nu\, v_t^2 \gg 1$, where D is constant for $v_1 \leq v_{||} \leq v_2$ and zero otherwise. Here D_{QL} is the quasilinear diffusion coefficient, ν is the bulk collision frequency, $v_t = (T_B/m_e)^{1/2}$, T_B is the bulk temperature and $v_1(v_2)$ is the low (high) velocity boundary of the resonant domain.

We find a strong enhancement in the perpendicular temperature in the resonant plateau, $T_\perp \gg T_B$.[1] An analytical formula shows that $T_\perp = T_\perp (v_1, v_2)$ in reasonable agreement with the numerical results over a wide range of parameters. As a result of this there are many more current carriers in the tail and the two-dimensional current density is much larger than the one indicated from a one-dimensional theory.[2] This contradicts previous findings,[3] but agrees qualitatively with our numerical integration.[4] The two-dimensional figure of merit $(J/P_d)_2$ is 3 times larger than the prediction of the one-dimensional theory. This is in excellent agreement both with Ref. 3 and our numerical work.[4]

b. Relativistic Theory of Lower-Hybrid (LH) Current Generation

An analytical treatment based on the method of moments is developed. The relativistic Fokker-Planck equation for energetic electrons colliding with a thermal background of electrons and ions is derived as the Landau limit of the relativistic Balescu-Lenard collision operator.[5,6] Subsequently the energy, velocity and momentum moments of the relativistic Fokker-Planck equation are taken in the presence of RF diffusion. Since one is mainly interested in the average parallel and perpendicular momentum of the current carrying electrons the simplest possible distribution, which conveys this information, is employed — namely, one that consists of a product of displaced delta functions. This procedure provides us with the evolution equations of the average energy, momentum and current of the energetic electrons with LH diffusion. These equations when solved for the steady state provide us with the relations among the power dissipated, average energy and current carried by the energetic electron. The figure of merit as well as the average perpendicular energy are also calculated.

A numerical code of the 2D Fokker-Planck equation with relativistic effects taken into account has also been developed.[4,7,8] The numerical results indicate a significant enhancement of the perpendicular temperature as well as of the radial one. The current generated, power dissipated and perpendicular temperature are more or less insensitive to changes of the diffusion coefficient in the regime of strong RF-diffusion. Current and power dissipated change significantly with the location of the RF spectrum in parallel phase velocity. Relativity also affects significantly the current generated and the power dissipated but the figure of merit is only slightly affected. A very good agreement between the numerical results[9] for the perpendicular temperature and the simple analytic relativistic theory has been found.

The relativistic Fokker-Planck equation combined with RF diffusion has also been solved for arbitrary values of RF diffusion coefficient under conditions of detailed balance of the stationary joint

distribution involved.[10] The solution is in a closed form and therefore easily amenable to various analyses (small or large diffusion coefficients, etc.) in calculating current generated and power dissipated. The detailed balance condition also provides useful information about the functional form of the diffusion coefficients which are associated with the existence of a stationary steady state. The latter is also associated with a saturated spectrum of fluctuations in a plasma driven by a LH spectrum.

c. Stochastic Heating and Current Generation by Localized RF Fields

We consider the momentum transfer and diffusion of electrons interacting with a coherent one-dimensional wavepacket. Such a problem arises, for example, in lower-hybrid current drive, where electrons moving on a magnetic field surface around the torus interact periodically with a wave during the crossings of the resonance cone. With an effective length of the torus ℓ and a width of the resonance cone d we have typically $\ell \gg$ d. This implies a large number of Fourier modes.

We consider an imposed field of such an amplitude that no particles from the bulk of the distribution are trapped. In that case the wave, maintained by the bulk particles, remains unchanged and we study the nonlinear dynamics of the high energy tail particles. The problem is treated both analytically and numerically. Earlier work on a similar problem is due to Stix[11] and Matsuda.[12]

For fields such that the autocorrelation time τ_{AC} is smaller than the trapping time τ_{TR} we find that the process is diffusive when the islands of neighboring Fourier modes overlap. The diffusion coefficient (D) is given essentially by the quasilinear formula, but with the important difference that only the overlapping modes should be included in calculating the r.m.s. field (E_{rms}) and τ_{AC}. With this modification we find an excellent agreement between theory and numerical experiments.[13,14] At larger amplitudes we find that D does not scales like E_{rms}^2. It does not follow the scaling of the resonance broadening theory, $\sim E_{rms}^{3/2}$, either. Depending on the width of the spectrum, the scaling is between $E_{rms}^{1/2}$ and E_{rms}. This numerical result should be explained by a theory for strong fields. In that case, we believe, the mechanism which leads to a diffusive motion is the crossing of the separatrices.

d. Induced Stochasticity by a Frequency-Modulated Wave

We have been studying the one-dimensional motion of an electron in a static confining potential and being perturbed by an electrostatic frequency modulated (fm) wave.[15] This problem models the motion of an electron along a d.c. magnetic field when it is confined by the field and an electrostatic potential. Such a situation would exist in the end-plugs of tandem mirror plasmas. The perturbing wave models an externally launched rf wave. The objective of this problem is to investigate the possibility of enhancing the electrostatic potential in the end-plugs by modifying the electron distribution function there so that the potential depends more favorably on the density than is given by the Boltzmann relation.

Our preliminary results[15] indicate that for very small amplitudes the fm-wave perturbs the electron

motion dramatically in regions of phase-space where the wave itself is not located. This happens for particular choices of the modulational index of the fm-wave and for frequencies which are close to the bounce frequency of the electron near the bottom of the confining potential. A large region of phase space can be driven stochastic by the fm-wave and the distribution function flattened in that region on a time-scale that is small compared to the electron-electron collisional time. The fm-wave can have its phase velocity far away in phase space so that it will not affect the passing electrons from the central cell. As an example, for TARA end-plug parameters, an fm-wave with an amplitude of 0.2 V/cm can flatten the electron distribution function for velocities, v, such that $0 \leq v \leq 2v_{te}$ (where v_{te} is the electron thermal velocity). This stochastic region of phase-space is nearly independent of the phase velocity, v_{ph}, of the wave as long as $v_{ph} \geq 2v_{te}$. This requires a frequency modulation of only 10% about the central carrier frequency — a spread that is easy to obtain experimentally.

e. Three-Dimensional Pulse Shapes of Absolute and Convective Instabilities for Relativistic Observers

The space-time growth and propagation of instabilities in a plasma is of considerable, general interest and has been recently reviewed.[16] The technique for distinguishing between absolute and convective instabilities is based upon the pinch-point analysis of the Green's function,[17] and the time asymptotic pulse shape of such instabilities is determined from the pinch points as seen by moving observers.[18] The latter was only developed for nonrelativistic observers and hence is, strictly speaking, applicable only to nonrelativistic plasma dynamics and unstable modes that propagate with velocities that are much smaller than the velocity of light, c (e.g., unstable electrostatic modes). We have recently generalized the pinch point analysis so that asymptotic pulse shapes can be obtained for relativistic-electromagnetic instabilities in three dimensions.[19,20] The following is a summary of our major results.

Let the dispersion relation, in the laboratory frame of reference, be $D(\vec{k},\omega) = 0$. For an observer moving with velocity $\vec{V}$ relative to the lab frame the Fourier-Laplace transform of the Green's function is then given by $D_V^{-1}(\vec{k}',\omega',\vec{V}) \equiv D^{-1}[\vec{k}'(\vec{k}',\omega',\vec{V});\ \omega(\vec{k}',\omega',\vec{V})]$ where the unprimed and primed quantities are related by well-known relativistic transformation equations.[21] The pinch-points $(\vec{k}'_0,\omega'_0)$ are the proper solutions of $D_V = 0$ and $(\partial D_V/\partial \vec{k}') = 0$. Their dependence upon $\vec{V}$ is given by the following differential equations:

$$\frac{\partial \omega'_0}{\partial \vec{V}} = -\gamma^2 \vec{k}'_{0\parallel} - \gamma \vec{k}'_{0\perp} \tag{18.1}$$

$$\delta\vec{k}'_0 \cdot \overleftrightarrow{G}' = \delta\vec{V} \cdot \overleftrightarrow{F} \tag{18.2}$$

where

$$\overleftrightarrow{G}' = \left(\frac{\partial}{\partial \vec{k}'_\perp} + \frac{\partial}{\partial \vec{k}'_\parallel}\right)\left(\frac{\partial}{\partial \vec{k}'_\perp} + \frac{1}{\gamma}\frac{\partial}{\partial \vec{k}'_\parallel}\right) D_v \tag{18.3}$$

$$\overleftrightarrow{F} = -\gamma \frac{\partial D_v}{\partial \omega'} \overleftrightarrow{\delta} - \left[\frac{\gamma \omega_o'}{c^2} \left(\frac{\partial}{\partial \vec{k}_\perp'} + \gamma \frac{\partial}{\partial k_{\parallel}'} \right) \right. \tag{18.4}$$

$$\left. + \frac{(\gamma - 1)}{V} \left(k_{\parallel}' \frac{\partial}{\partial \vec{k}_\perp'} - \vec{k}_\perp' \frac{\partial}{\partial k_{\parallel}'} \right) \right] \left(\frac{\partial}{\partial \vec{k}_\perp'} + \frac{1}{\gamma} \frac{\partial}{\partial \vec{k}_{\parallel}'} \right) D_v$$

$\gamma = [1 - (V^2/c^2)]^{-1/2}$, and all derivative operators are to be evaluated at the pinch-point $(\vec{k}_0', \omega_0')$. The time-asymptotic pulse shape is then obtained from the plot of $[(\max \omega_{oi}')/\gamma]$ vs. $\vec{V}$, where $(\max \omega_{oi}')$ is the maximum imaginary part pinch-point frequency.

Alternatively, in the laboratory frame of reference the pinch points $(\vec{k}_0', \omega_0')$ have corresponding values $(\vec{k}_0, \omega_0)$. As a function of $\vec{V}$, $(\vec{k}_0, \omega_0)$ are determined by the pinch-point solutions of $D = 0$ and $(\partial D/\partial \vec{k}_\perp) + \gamma(\partial D/\partial \vec{k}_{\parallel}) + \gamma \vec{V}(\partial D/\partial \omega) = 0$. They obey the following, simpler differential equations:

$$\frac{\partial \omega_o}{\partial \vec{V}} = -\frac{\partial D}{\partial \omega} \left[\overleftrightarrow{T} \right]^{-1} \cdot \vec{V} \tag{18.5}$$

$$\delta \vec{k}_o \cdot \overleftrightarrow{T} = -\frac{\partial D}{\partial \omega} \delta \vec{V} \tag{18.6}$$

where

$$\overleftrightarrow{T} = \left(\frac{\partial}{\partial \vec{k}} + \vec{V} \frac{\partial}{\partial \omega} \right)^2 D \tag{18.7}$$

and the derivative operators are evaluated at $(\vec{k}_o, \omega_o)$. For any fixed $(\vec{r}/t) = \vec{V}$ the time-asymptotic Green's function is proportional to $t^{-3/2} \exp[i(\vec{k}_o \cdot \vec{V} - \omega_o)t]$, and, its logarithmic magnitude is thus given by $(-\vec{k}_{oi} \cdot \vec{V} + \omega_{oi})t = \omega_{oi}' t' = (\omega_{oi}'/\gamma)t$. The time-asymptotic pulse shape is hence again determined from $[(\max \omega_{oi}')/\gamma]$ as a function of $\vec{V}$.

f. Relativistic-Electromagnetic Instabilities at Electron Cyclotron Harmonics

The analysis of absolute and convective instabilities[16-18] has been generalized for application to relativistic and fully electromagnetic instabilities in plasmas.[19,20] In particular, we have applied our analysis to electromagnetic instabilities propagating along a constant magnetic field,[19,22] $(\vec{B}_0)$, in which the plasma is immersed, as well as to those propagating perpendicular to $\vec{B}_0$.[20] These instabilities are driven by a highly anisotropic distribution function of relativistic electrons. Such a situation is found to be relevant in explaining the observed nonthermal radiation in the ECRH plasmas on TMX-Upgrade.[23] Our model analysis for waves along $\vec{B}_0$[19,22] shows that two distinct instabilities exist — the whistler instability and the relativistic instability. The former may be stabilized by introducing a thermal spread in the distribution function while the latter can only be stabilized by

increasing the density. For waves propagating perpendicular to $\vec{B}_0$,[20] electromagnetic instabilities occur at harmonics of the electron cyclotron frequency (ω_{ce}). The nature and the strength of the instabilities is highly sensitive to the plasma density. For low densities the dominant instability is at ω_{ce}. It is an absolute instability and its phase-velocity is greater than the speed of light (c). The instabilities at harmonics of ω_{ce} are convective in nature. As the density is increased the phase velocity of the instability at ω_{ce} becomes less than c while it still remains absolute. However, the instability at $2\omega_{ce}$ has the highest growth rate. It becomes an absolute instability with its phase velocity less than c.

References

1. V. Krapchev, D. Hewett, and A. Bers, "Steady State Solution of a 2D Fokker-Planck Equation with Strong RF Diffusion," M.I.T. Plasma Fusion Center Report PFC/JA-83-32; V. Krapchev, D. Hewett, and A. Bers, "Steady State Solution of a Two-Dimensional Fokker-Planck Equation with Strong RF Diffusion," Bull. Amer. Phys. Soc. 28, 1090 (1983); V. Krapchev, D. Hewett, and A. Bers, "Analytic Solution of the 2D Fokker-Planck Equation for LH Current Drive," US-Japan Workshop on RF Heating and Current Generation, GA Technologies, Inc., San Diego, California, 1983.
2. N.J. Fisch, Phys. Rev. Lett. 41, 873 (1978).
3. C.F.F. Karney and N.J. Fisch, Phys. Fluids 22, 1817 (1979).
4. D. Hewett, K. Hizanidis, V. Krapchev, and A. Bers, "Two-Dimensional and Relativistic Effects in Lower-Hybrid Current Drive," Proceedings of the IAEA Technical Committee on the Non-Inductive Current Drive in Tokamaks, Culham, England, April 1983, Culham Report CLM-CD, 1983; D. Hewett, V. Krapchev, J. Freidberg, and A. Bers, "Fokker-Planck Investigations of RF Current Drive," Sherwood Theory Meeting, Arlington, Virginia, 1983; M. Shoucri, V. Krapchev, and A. Bers, "A SADI Numerical Scheme for the Solution of the 2-D Fokker-Planck Equation," IEEE International Conference on Plasma Science, San Diego, California, 1983.
5. K. Hizanidis, K. Molvig, and K. Swartz, J. Plasma Physics 32, 223 (1983).
6. V.P. Silin, Sov. Phys. JETP 13, 1244 (1961).
7. K. Hizanidis, V. Krapchev, and A. Bers, "Relativistic Two-Dimensional Theory of RF Current Drive," Proceedings of the Fifth Topical Conference on Radio Frequency Plasma Heating, Madison, Wisconsin, February 1983.
8. K. Hizanidis, D.W. Hewett, K. Rugg, and A. Bers, "Steady State RF-Current Drive Theory Based Upon the Relativistic Fokker-Planck Equation," Bull. Amer. Phys. Soc. 28, 8, 1090 (1983).
9. K. Hizanidis, D.W. Hewett, and A. Bers, "Solution of the Relativistic 2-D Fokker-Planck Equation for LHCD," US-Japan Workshop on RF Heating and Current Generation, GA Technologies, Inc., San Diego, California, 1983; K. Hizanidis, V. Krapchev, and A. Bers, "Relativistic 2-Dimensional Theory of Lower-Hybrid Current Drive," Sherwood Theory Meeting, Arlington, Virginia, 1983.
10. H. Risken, Z. Physik 251, 231 (1972), and references therein.
11. T.H. Stix, Proceedings of the Joint Varenna-Grenoble International Symposium on Heating in Toroidal Plasmas 2, 363 (1978).
12. K. Matsuda, Reports GA-A16303 (1980), GA-15816 (1981).
13. V. Fuchs, V. Krapchev, A. Ram, and A. Bers, "Diffusion of Electrons by Coherent Wavepackets," M.I.T. Plasma Fusion Center Report PFC/JA-83-26, Physica D Nonlinear Phenomena, accepted for publication.
14. V. Fuchs, V. Krapchev, A. Ram, and A. Bers, "Stochasticity Induced by Coherent Wavepackets," Proceedings of the Fifth Topical Conference on Radio Frequency Plasma Heating, Madison,

Wisconsin, February 1983; V. Fuchs, V. Krapchev, A. Ram, and A. Bers, "Scattering and Stochasticity of Electrons Interacting with Coherent Wavepackets," Sherwood Theory Meeting, Arlington, Virginia, 1983.
15. A. Ram, M. Mauel, V. Krapchev, and A. Bers, Bull. Amer. Phys. Soc. 28, 1183 (1983).
16. A. Bers, "Space-Time Evolution of Plasma Instabilities — Absolute and Convective," in M.N. Rosenbluth and R.Z. Sagdeev (Gen. Eds.), Handbook of Plasma Physics; A.A. Galeev and R.N. Sudan (Vol. Eds.), Vol. 1, Basic Plasma Physics, Chapter 3.2, (North Holland Publishing Co. 1983).
17. R.J. Briggs, Electron Stream Interaction with Plasmas, (M.I.T. Press 1964).
18. L.S. Hall and W. Heckrotte, Phys. Rev. 166, 120 (1968).
19. A. Bers and A. K. Ram, "Relativistic Pulse Shapes of Absolute and Convective Instabilities," Bull. Am. Phys. Soc. 27, 919 (1982).
20. A. Bers, A. Ram, and G. Francis, "Relativistic Stability Analysis of Electromagnetic Waves Propagating Across a Magnetic Field," Bull. Amer. Phys. Soc. 28, 1158 (1983).
21. A. Bers, "Linear Waves and Instabilities," in C. DeWitt and J. Peyraud (Eds.), Plasma Physics — Les Houches 1972, (Gordon and Breach Science Publishers 1975), p.134.
22. A. Ram and A. Bers, Annual Sherwood Controlled Fusion Conference, Arlington, Virginia, 1983.
23. Y.J. Chen, W.M. Nevins, and G.R. Smith, LLNL, private communication.

Other Publications

Bers, A. and K.S. Theilhaber, "Three-Dimensional Theory of Waveguide-Plasma Coupling," Nucl. Fusion 23, January 1983.

Fuchs, V., M.M. Shoucri, G. Thibaudeau, L. Harten, and A. Bers, "High-Q Thermally Stable Operation of a Tokamak Reactor," IEEE Trans. on Plasma Science PS-11, 4 (1983).

Ram, A., and A. Bers, "Antenna-Plasma Coupling Theory for ICRF Heating," Proceedings of the Fifth Topical Conference on Radio Frequency Plasma Heating, Madison, Wisconsin, February 1983 and M.I.T. Plasma Fusion Center Report PFC/CP-83-1 (1983).

Ram, A., and A. Bers, "Coupling Theory for ICRF Heating of Large Tokamaks," Nucl. Fusion, accepted for publication in 1984; M.I.T. Plasma Fusion Center Report PFC/JA-83-40 (1983)

18.6 Physics of Thermonuclear Plasmas

U.S. Department of Energy (Contract DE-AC02-78ET-51013)

Bruno Coppi

The general objective of this program is the theoretical study of plasmas in thermonuclear regimes and it extends from the design of "burning core" experiments for both D-T and advanced fuel reactors to the basic study of plasma transport and stability questions. Continuous collaboration and theoretical guidance are provided for the Alcator and Versator experimental programs that involve high density regimes, with record values of the confinement parameter, as well as low and intermediate density regimes where current drive and r.f. heating can be produced. Much of the support involves the development, modification, and use of realistic simulation codes that are among the most advanced in the research community, particularly in the transport and r.f. areas.

Other areas of interest in which considerable progress has been made in 1983 are: the theoretical

explanation and description of enhanced electron and ion thermal conductivity observed in present day experiments and its relevance to future ones in which heating due to the fusion reaction products will prevail; the particle transport processes that occur in high density plasmas with either neutral gas (so-called "puffing") or pellet injection; the identification and analysis of heating sequences from low to high-β regimes (β being the ratio of particle pressure to magnetic pressure) that remain macroscopically stable; and the implications of these sequences for future reactor concepts and new types of experiments, such as PBX, that have been proposed since we have pointed out the theoretical possibility to reach relatively high values of β by exploiting the favorable factors that lead to the "second stability region"; the excitation of internal macroscopic modes by the fusion reaction products and their influence on the time needed to reach ignition; the relevant stability analysis of collisionless modes that involve magnetic reconnection; the investigation of new physical processes to make the experimental study of advanced fuel (such as D-D and D-He^3) burning feasible within the limits of present day technology; the burning conditions of plasmas with spin polarized nuclei, the collective modes that can be excited in them and the relevance that some of these modes have to ion cyclotron heating, to anomalous slowing down of the charged fusion reaction products and to the rate of spin depolarization.

As is traditional with our mode of operation, during 1983 we have maintained an effective system of close collaborations with national and overseas institutions for both our theoretical and experimental program. Our contributions have been presented at major national and international meetings.